

A new locally mass conserving, monotonic and accurate method for solving the continuity equations in Earth System Models



Second International Conference on Earth System Modelling - Hamburg 2007.

Eigil Kaas, University of Copenhagen (kaas@gfy.ku.dk)

Abstract

To correctly simulate the evolution and interactions of chemical constituents in Earth System Models it is important that the algorithms of the underlying dynamical core fulfill a number of properties such as high order of accuracy, inherent mass conservation, locality, positive definiteness, monotonicity, consistency, and high order of numerical stability and efficiency. Furthermore the so-called mass-wind inconsistency problem should be minimised in a physically consistent way. Aiming at fulfilling all these requirements simultaneously a new scheme has been introduced. It is based on two new ingredients:

1) a simple and cost effective method to ensure local, i.e. inherent, mass conservation in traditional semi-implicit (SI), semi-Lagrangian (SL) models

2) an efficient locally mass conserving spatial filter.

The basic mass conserving SL method is relatively simple to construct from existing SL general circulation models. The trick is to introduce weights at the upstream departure points ensuring that the total mass given by a given Eulerian grid point to the surrounding SL departure points is equal to the volume represented by that grid point. Based on the Eulerian grid point weights it is possible to obtain departure point weights representing the divergence associated with the SL trajectories as in the so-called cell-integrated semi-Lagrangian (CISL) models.

The filter is simple but it efficiently ensures monotonicity and positive definiteness and surprisingly it enhances the accuracy. Furthermore it can be constructed to generally maintain constancy in non-divergent flows.

So far the scheme has only been tested in traditional two dimensional advection tests and in a semi-Lagrangian, semi-implicit shallow water model in plain geometry but with topography. Without the filter the scheme is at least as accurate as the traditional SL schemes. The filter enhances the accuracy for all tests carried out. However, it becomes particularly impressive near sharp gradients and discontinuities.

The increase in numerical cost of the new scheme relative to traditional SI-SL models is small, particularly when there are several passive tracers

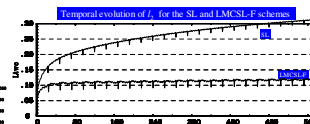
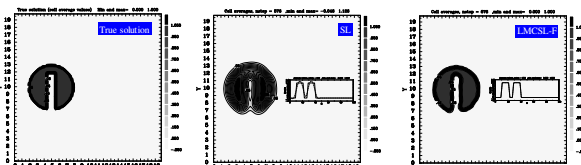
Idealised passive advection tests

Error measures:

$$rms = \sqrt{\frac{1}{K} \sum_{i=1}^K (\psi_i - \psi_i^*)^2}, \quad l_1 = \frac{\sum_{i=1}^K |\psi_i - \psi_i^*|}{\sum_{i=1}^K |\psi_i|}, \quad l_2 = \frac{\sqrt{\sum_{i=1}^K (\psi_i - \psi_i^*)^2}}{\sqrt{\sum_{i=1}^K \psi_i^2}}, \quad L_\infty = \frac{\max(|\psi_i - \psi_i^*|)}{\max(|\psi_i|)}$$

$$h_{max} = \frac{\max(\psi) - \max(\psi^*)}{S'} \quad \text{and} \quad h_{min} = \frac{\min(\psi) - \min(\psi^*)}{S'} \quad \text{with} \quad S' = \max(\psi') - \min(\psi')$$

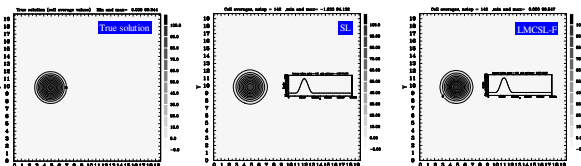
Slotted cylinder (101x101 points, 6 full rotations (576 time steps):



Scheme	Resolution	rms	l1	l2	L_infinity	h_max	h_min
BioSL	51x51	0.1107	0.7407	0.5055	0.6802	-2.81e-00	-6.3E-01
BioSL	101x101	0.0701	0.3651	0.3079	0.6674	0.12E+00	-4.7E-01
BioSL	151x151	0.0504	0.2445	0.2455	0.6816	0.11E+00	-1.3E+00
BioSL	201x201	0.0492	0.2000	0.2122	0.6549	0.11E+00	-1.3E+00
LMCSL-F	51x51	0.0713	0.2624	0.3225	0.8531	-7.9E-01	-1.3E+00
LMCSL-F	101x101	0.0225	0.0619	0.0988	0.5481	0.21E+00	-1.0E+00
LMCSL-F	151x151	0.0166	0.0383	0.0721	0.3179	0.21E+00	-2.0E+00
LMCSL-F	201x201	0.0142	0.0293	0.0615	0.3214	0.35E+04	-1.8E+00

Table 1. Slotted cylinder experiment after six full rotations (576 time steps). BioSL: a traditional semi-Lagrangian scheme and LMCSL-F: the corresponding locally mass conserving scheme plus the monotonic filter.

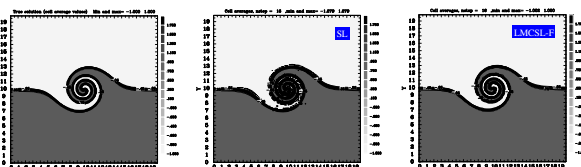
Cosine hill (65x65 points, 2 full rotations (142 time steps):



Scheme	Resolution	rms	l1	l2	L_infinity	h_max	h_min
BioSL	33x33	0.2643	0.4928	0.2026	0.6205	-3.5E+00	-2.0E+01
BioSL	65x65	0.2029	0.3073	0.2040	0.2048	-3.6E+00	-5.0E+00
BioSL	97x97	0.1305	0.2185	0.0821	0.5792	-3.9E+00	-3.0E+00
BioSL	129x129	0.0502	0.0971	0.0663	0.2045	-1.7E+00	-2.0E+00
LMCSL-F	33x33	0.2703	0.5749	0.0971	1.1297	-3.0E+00	-6.5E+00
LMCSL-F	65x65	0.2041	0.2981	0.0649	0.2091	-3.0E+00	-3.9E+00
LMCSL-F	97x97	0.2023	0.0702	0.0651	0.4179	-1.3E+00	-1.8E+00
LMCSL-F	129x129	0.0143	0.0201	0.0330	0.5069	-0.75E+00	-3.9E+00

Table 2. As table 1. But for the cosine hill problem and with time step: full rotation.

Cyclogenesis (129x129 points, 16 time steps):



Scheme	Resolution	rms	l1	l2	L_infinity	h_max	h_min
BioSL	33x33	0.1204	0.0398	0.2109	0.0800	0.43E+01	-4.1E+01
BioSL	65x65	0.0647	0.0193	0.0657	0.0771	0.42E+01	-6.2E+01
BioSL	97x97	0.0496	0.0130	0.0502	0.0476	0.83E+01	-8.3E+01
BioSL	129x129	0.0418	0.0101	0.0422	0.3609	0.75E+01	-7.5E+01
LMCSL-F	33x33	0.0938	0.0271	0.1017	0.3978	0.70E+00	-3.7E+00
LMCSL-F	65x65	0.0487	0.0111	0.0458	0.4142	0.07E+00	-2.7E+00
LMCSL-F	97x97	0.0345	0.0070	0.0349	0.5241	0.84E+00	-7.6E+00
LMCSL-F	129x129	0.0264	0.0041	0.0266	0.4822	0.12E+02	-1.1E+02

Table 3. As table 1. But for the cyclogenesis problem (16 time steps).

Traditional semi-Lagrangian (SL) scheme: Passive advection in divergent flow

Explicit forecast in grid point k :

$$\psi_k^{n+1} = \sum_{i=1}^K w_{k,i} (\psi_i^n - 0.5 \Delta t (\nabla \cdot \mathbf{v})_i^n) - 0.5 \Delta t (\nabla \cdot \mathbf{v})_k^{n+1}$$

k Grid point/cell index, $k = 1, \dots, K$, $K = nlon \cdot nlat$

l Grid point/cell index, $l = 1, \dots, K$

$w_{k,l}$ Weights on upstream departure grid points representing the polynomial upstream interpolations. These weights are only different from zero in Eulerian points l close to the semi-Lagrangian departure point.

Per definition we have $\sum_{i=1}^K w_{k,i} = 1$

$(\tilde{\psi})^{n+1}$ Extrapolated value $(\tilde{\psi})^{n+1} = 2(\tilde{\psi})^n - (\tilde{\psi})^{n-1}$

Locally mass conserving semi-Lagrangian (LMCSL) scheme: Passive advection in divergent flow

Explicit forecast in grid point i :

$$\psi_i^{n+1} = \sum_{j=1}^K \hat{w}_{i,j} \psi_j^n \quad \text{where} \quad \hat{w}_{i,j} = \frac{A_j w_{i,j}}{\sum_{m=1}^K A_m w_{i,m}}$$

A_k Volume represented by the k th Eulerian grid point.

Mass is (locally) conserved:

$$\sum_{i=1}^K A_i \psi_i^{n+1} = \sum_{i=1}^K \sum_{j=1}^K A_i \hat{w}_{i,j} \psi_j^n = \sum_{i=1}^K \sum_{j=1}^K \frac{A_i w_{i,j}}{\sum_{m=1}^K A_m w_{i,m}} \psi_j^n = \sum_{j=1}^K \sum_{i=1}^K \frac{A_i w_{i,j}}{\sum_{m=1}^K A_m w_{i,m}} \psi_j^n = \sum_{j=1}^K A_j \psi_j^n$$

Divergence is defined implicitly from the weighted weights, i.e. by the trajectories:

$$\partial_{t_i} = \frac{1}{\Delta t} \left(1 - \sum_{j=1}^K \hat{w}_{i,j} \right)$$

Monotonic and positive definite filter

Input to filter:

- A high order (bi-cubic interpolation) LMCSL unfiltered forecast ψ_j .
- A low order (bi-linear interpolation) LMCSL unfiltered forecast ψ_j .
- A maximum (ψ_{max}) and minimum (ψ_{min}) value permitted in each grid cell. This is defined from the maximum and minimum values of the four upstream grid points surrounding the semi-Lagrangian departure point, modified by the effect of divergence/convergence. This is taken into account using the traditional centered difference definition of divergence, implying that the filter ensures conservation of a constant field in non-divergent flows.

The filter:

- Set target values ψ_j equal to ψ_j .
- Identify grid cells where $\psi_j \notin [\psi_{min}, \psi_{max}]$. In these and in the eight neighboring grid cells a mask is set.
- In the masked cells a modified anti-filtered target value is set: $\psi_j = \psi_j + a(\psi_j - \psi_j)$ with $a = \min(1.6, 1 + 25 \cdot \text{abs}(\psi_j - \psi_j)/r)$ and $r = \max(\psi_j - \min(\psi_j))$.
- In the masked cells the ψ_j values are reset as $\min(\psi_{max}, \max(\psi_{min}, \psi_j))$ to ensure shape conservation.
- The ψ values in 2×2 complementary grid cell domains covering the total integration domain are modified to ensure new ψ values which are as close as possible to ψ_j under the strong constraint of local conservation of total mass in the four grid cells and the weak constraint of limitation to the individual grid cell intervals $[\psi_{min}, \psi_{max}]$.
- The above step is repeated for the set of 2×2 complementary grid cell domains that provide maximum spatial overlaps with the domains in the previous step.
- A final check and correction for violation of $\psi \in [\psi_{min}, \psi_{max}]$ is done on slightly larger grid cell domains (up to 13×13 grid cells) surrounding the violating cell using the same procedure used above for the 2×2 domains. This step only becomes active around very few – if any – violating cells.

Application to the shallow water equations and the semi-implicit technique

$$\begin{aligned} \frac{du}{dt} &= f v - \frac{d(\phi + \phi_p)}{dx} \\ \frac{dv}{dt} &= -f u - \frac{d(\phi + \phi_p)}{dy} \\ \frac{d\phi}{dt} &= -\phi D + F_p, \quad D = \nabla \cdot \mathbf{v} = \frac{du}{dx} + \frac{dv}{dy} \\ \frac{d\psi}{dt} &= -\psi D \end{aligned}$$

where $\begin{cases} \phi = gh, & h \text{ is depth of fluid} \\ \phi_p = gh_p, & h_p \text{ is height of topography} \\ u, v & \text{velocity components} \\ F_p & \text{Newtonian cooling (driving the model)} \\ \psi & \text{density of passive tracer} \end{cases}$

The LMCSL scheme can be combined with the semi-implicit resulting in a numerically stable dynamical model. Here we use the LMCSL scheme both for the geopotential height field and for a passive tracer (on-line coupling).

